

## Thin Films of Highly Luminescent Lanthanide Complexes Covalently Linked to an Organic–Inorganic Hybrid Material via 2-Substituted Imidazo[4,5-f]-1,10-phenanthroline Groups

Philip Lenaerts,<sup>†</sup> Annick Storms,<sup>‡</sup> Jules Mullens,<sup>‡</sup> Jan D'Haen,<sup>§,||</sup>  
Christiane Görller-Walrand,<sup>†</sup> Koen Binnemans,<sup>†</sup> and Kris Driesen<sup>\*,†</sup>

Department of Chemistry, Katholieke Universiteit Leuven, Celestijnenlaan 200F, B-3001 Leuven, Belgium,  
Laboratory of Inorganic and Physical Chemistry, Department SBG, Hasselt University, Agoralaan,  
Building D, B-3590 Diepenbeek, Belgium, Institute for Materials Research, Hasselt University,  
Wetenschapspark 1, B-3590 Diepenbeek, Belgium, and IMEC vzw, division IMOMECE, Wetenschapspark 1,  
B-3590 Diepenbeek, Belgium

Received May 30, 2005. Revised Manuscript Received July 13, 2005

A homogeneous distribution of luminescent lanthanide(III) 2-thenoyltrifluoroacetate complexes (Ln = Pr, Nd, Sm, Eu, Dy, Ho, Er, Tm, Yb) in an organic–inorganic hybrid material was obtained by grafting the complexes to the solid matrix via 2-substituted imidazo[4,5-f]-1,10-phenanthroline moieties. Thin films of the silica hybrid material were prepared by the sol–gel method and by spin-coating of the gelating solution on glass slides or on oxidized silicon wafers. The thickness of the thin films was determined by scanning electron microscopy (SEM). High-resolution luminescence spectra of the lanthanide complexes were recorded, and the luminescence decay times were measured. The luminescence quantum yields of europium(III)-doped thin films exposed to different drying conditions were determined by using an integrating sphere.

### Introduction

The trivalent lanthanide ions are well-known for their photoluminescence properties in the visible and near-infrared regions. Due to the poor absorption abilities of the lanthanide ions, it is common practice to form complexes of the lanthanide ions with organic ligands that strongly absorb light and transfer the energy to the metal center (antenna effect).<sup>1–9</sup> In addition, the ligands expel water from the first coordination sphere, which can cause radiationless deactivation.<sup>10,11</sup> To explore the potential of the complexes for photonic applications (light-converting devices),<sup>12–17</sup> it is useful to

incorporate the complexes in an inert host matrix.<sup>18–27</sup> A problem often encountered upon embedding of the luminescent complexes in the host matrix is the nonhomogeneous distribution of the compounds,<sup>28,29</sup> which leads to clustering of lanthanide ions and hence a decrease of the luminescence intensity.<sup>30,31</sup> A more homogeneous distribution of the lanthanide complex in the host matrix can be achieved by covalent coupling of the complexes to this host matrix.<sup>32–39</sup> In our previous work, we used 5-amino-1,10-phenanthroline

\* Corresponding author. Phone: +32-16-327446 Fax: +32-16-327992. E-mail: Kris.Driesen@chem.kuleuven.be.

<sup>†</sup> Katholieke Universiteit Leuven.

<sup>‡</sup> Laboratory of Inorganic and Physical Chemistry, Hasselt University.

<sup>§</sup> Institute for Materials Research, Hasselt University.

<sup>||</sup> IMEC vzw.

- Weissman, S. I. *J. Chem. Phys.* **1942**, *10*, 214.
- Forsberg, J. H. *Gmelin Handbook of Inorganic Chemistry, Sc, Y, La–Lu Rare Earth Elements*; Springer-Verlag: Berlin, 1981; System No. 39, Vol. D3, pp 65–251 and references therein.
- Melby, L. R.; Rose, N. J.; Abramson, E.; Caris, J. C. *J. Am. Chem. Soc.* **1964**, *86*, 5117.
- Drake, S. R.; Lyons, A.; Otway, D. J.; Slwain, A. M. Z.; Williams, D. J. *J. Chem. Soc., Dalton Trans.* **1993**, *15*, 2379.
- Wang, C. Y.; Yang, Z. J.; Li, Y.; Gong, L. W.; Zhao, G. W. *Phys. Status Solidi A* **2002**, *191*, 117.
- Zhong, G. L.; Kim, K.; Jin, J. I. *Synth. Met.* **2002**, *129*, 193.
- Adachi, C.; Baldo, M. A.; Forrest, S. R. *J. Appl. Phys.* **2000**, *87*, 8049.
- Sano, T.; Fujita, M.; Fujii, T.; Hamada, Y.; Shibata, K.; Kuroki, K. *Jpn. J. Appl. Phys.* **1995**, *34*, 1883.
- Li, H. H.; Inoue, S.; Machida, K.; Adachi, G. *Chem. Mater.* **1999**, *11*, 3171.
- Haas, Y.; Stein, G. *J. Phys. Chem.* **1971**, *75*, 3677.
- Stein, G.; Wurzburg, E. *J. Chem. Phys.* **1975**, *62*, 208.
- Kido, J.; Nagai, K.; Ohashi, Y. *Chem. Lett.* **1990**, 657.
- Kido, J.; Okamoto, Y. *Chem. Rev.* **2002**, *102*, 2357.
- Borzechowska, M.; Trush, V.; Turowska-Tyrk, I.; Amirhanov, W.; Legendziewicz, J. *J. Alloys Compd.* **2002**, *341*, 98.

- Kozanecki, A.; Sealy, B. J.; Homewood, K. *J. Alloys Compd.* **2000**, *300*, 61.
- Viana, B.; Koslova, N.; Aschehoug, P.; Sanchez, C. *J. Mater. Chem.* **1995**, *5*, 719.
- Strek, W.; Pawlik, E.; Deren, P.; Bednarkiewicz, A.; Wojcik, J.; Gaishun, V. E.; Malashkevich, G. I. *J. Alloys Compd.* **2000**, *300*, 459.
- Yang, C. Y.; Srdanov, V.; Robinson, M. R.; Bazan, G. C.; Heeger, A. J. *Adv. Mater.* **2002**, *14*, 980.
- Kuriki, K.; Koike, Y.; Okamoto, Y. *Chem. Rev.* **2002**, *102*, 2347.
- Wolff, N. E.; Pressley, R. J. *Appl. Phys. Lett.* **1963**, *2*, 152.
- Tanner, P. A.; Yan, B.; Zhang, H. J. *J. Mater. Sci.* **2000**, *35*, 4325.
- Bekiar, V.; Pistolis, G.; Lianos, P. *Chem. Mater.* **1999**, *11*, 3189.
- Li, H.; Inoue, S.; Machida, K.; Adachi, G. *Chem. Mater.* **1999**, *11*, 3171.
- Strek, W.; Sokolnicki, J.; Legendziewicz, J.; Maruszewski, K.; Reisfeld, R.; Pavich, T. *Opt. Mater. (Amsterdam)* **1999**, *13*, 41.
- Matthews, L. R.; Kobbe, E. T. *Chem. Mater.* **1993**, *5*, 1697.
- Costa, V. C.; Vasconcelos, W. L.; Bray, K. L. *J. Sol-Gel Sci. Technol.* **1998**, *13*, 605.
- Klonkowski, A. M.; Lis, S.; Pietraszkiewicz, M.; Hnatejko, Z.; Czarnobaj, K.; Elbanowski, M. *Chem. Mater.* **2003**, *15*, 656.
- Li, H. R.; Fu, L. S.; Lin, J.; Zhang, H. J. *Thin Solid Films* **2002**, *416*, 197.
- Du, C. X.; Ma, L.; Xu, Y.; Li, W. L. *J. Appl. Polym. Sci.* **1997**, *66*, 1405.
- Strek, W.; Legendziewicz, J.; Lukowiak, E.; Maruszewski, K.; Sokolnicki, J.; Boiko, A. A.; Borzechowska, M. *Spectrochim. Acta, Part A* **1998**, *54*, 2215.
- Wang, Q. M.; Yan, B. *J. Mater. Chem.* **2004**, *14*, 2450.
- Binnemans, K.; Lenaerts, P.; Driesen, K.; Görller-Walrand, C. *J. Mater. Chem.* **2004**, *14*, 191.

as a starting compound to attach a lanthanide complex to the host matrix.<sup>32,38,39</sup> Although the approach was successful, the synthesis of the 5-amino-1,10-phenanthroline is rather cumbersome, and there were some disadvantages such as the low stability of this compound. In this paper, we show that a 2-substituted imidazo[4,5-*f*]-1,10-phenanthroline is an easily accessible, stable, and versatile building block for covalent attachment of lanthanide  $\beta$ -diketonate complexes to a hybrid matrix. Bulk samples and thin films of lanthanide(III) 2-thenoyltrifluoroacetate complexes (Ln = Pr, Nd, Sm, Eu, Dy, Ho, Er, Tm, Yb) grafted via the imidazo[4,5-*f*]-1,10-phenanthroline moiety to the silica hybrid matrix were prepared. The thin films were studied by scanning electron microscopy (SEM). Luminescence spectra of the lanthanide complexes were recorded, and the luminescence lifetimes were measured. The quantum yields of europium(III)-doped thin films were determined by using an integrating sphere.

### Experimental Section

**General Procedures.** CHN elemental analyses were performed on a CE Instruments EA-1110 elemental analyzer. <sup>1</sup>H NMR spectra were recorded on a Bruker Avance 300 spectrometer (300 MHz). <sup>13</sup>C NMR spectra were recorded on a Bruker AMX 400 (100 MHz). Mass spectra were taken on a Thermo Finnigan LCQ Advantage mass spectrometer. FTIR spectra were recorded on a Bruker IFS-66 spectrometer, using the KBr pellet method. Photoluminescence spectra in the visible region have been recorded on an Edinburgh Instruments FS900 steady-state spectrofluorimeter. This instrument is equipped with a 450 W xenon arc lamp as the steady-state excitation source, an excitation monochromator (1800 lines mm<sup>-1</sup>), an emission monochromator (1800 lines mm<sup>-1</sup>), a microsecond flashlamp (pulse length 2  $\mu$ s), and a red-sensitive photomultiplier (300–850 nm). The steady-state luminescence spectra and the lifetime measurements in the infrared region were measured on an Edinburgh Instruments FS920P near-infrared spectrometer, with a 450 W xenon lamp, a double excitation monochromator (1800 lines mm<sup>-1</sup>), an emission monochromator (600 lines mm<sup>-1</sup>), and a liquid-nitrogen-cooled Hamamatsu R5509-72 near-infrared photomultiplier tube. For the lifetime measurements, the setup includes a Continuum Minilite II Nd:YAG laser which allows laser excitation of the sample at 1064, 532, 355, and 266 nm. The repetition rate is 10 Hz, and the pulse width is 3–5 ns. The luminescence lifetime has been determined by measurement of the luminescence decay curve. Measurement of the decay rate of the excited-state lifetimes in the visible region are subject to an experimental error of  $\pm 5\%$ , and in the near-infrared region an error of  $\pm 10\%$  is estimated. All photoluminescence spectra were recorded at room temperature, except for the sol-gel glass doped with praseodymium(III). This sample was cooled to 77 K in an Oxford Instruments OptistatDN nitrogen bath cryostat. The electronic transitions were assigned by

comparing the transitions in our spectra with those reported by Carnall et al.<sup>40</sup> for trivalent lanthanide ions in the host matrix LaF<sub>3</sub>, by Davey et al. for trivalent lanthanide ions in fluorozirconate glasses<sup>41</sup> and by other previous studies.<sup>42,43</sup> The spectra were corrected for variations in the output of the excitation source and for variations in the detector response.

The quantum yield of the europium(III)-doped thin films were determined using an integrating sphere (150 mm diameter, BaSO<sub>4</sub> coating) of Edinburgh Instruments. The spectra were corrected. The quantum yield can be defined as the integrated intensity of the luminescence signal divided by the integrated intensity of the absorption signal. Only the intense luminescence band of the <sup>5</sup>D<sub>0</sub>  $\rightarrow$  <sup>7</sup>F<sub>2</sub> transition around 612 nm was measured by the integrating sphere, but this intensity value was corrected by taking into account the relative intensity of the other transitions (as determined from the steady-state luminescence spectrum in the 550 nm–750 nm region). In this way, an intensity value that corresponds to the total luminescence output was obtained. The absorption intensity was calculated by subtracting the integrated intensity of the light source with the sample in the integrating sphere, from the integrated intensity of the light source with a blank sample in the integrating sphere. A solution of [Eu(tta)<sub>3</sub>(phen)] in DMF with known quantum yield (36.5%) was used as the reference.<sup>44</sup> Two similar cuvettes were used for both the solid sample (which was placed inside the cuvette) and the reference solution. Care was taken to obtain a reproducible placement of the cuvettes in the integration sphere. The quantum yield was determined by averaging at least 3 measurements. Thin films have been prepared by spin-coating on glass slides or on oxidized silicon wafers (SiO<sub>2</sub> layer: 300 nm) using a Polos MCD (manual chemical dispense) single wafer spin processor. The speed was set at 2000 rpm. Layer thickness of the thin films has been characterized on the cross-sections by means of SEM (Philips XL30-FEG) with an acceleration voltage of 15 kV.

1,10-Phenanthroline monohydrate, diethoxydimethylsilane (DEDMS), 3-glycidoxypropyltrimethoxysilane (GLYMO), 4-hydroxybenzaldehyde, and 2-thenoyltrifluoroacetone were purchased from ACROS Organics, 3-(triethoxysilyl)propyl isocyanate was purchased from ABCR Gelest, and tetramethoxysilane (TMOS) was purchased from Fluka. The lanthanide salts were obtained from Aldrich.

**Synthetic Procedures.** *Synthesis of 1,10-Phenanthroline-5,6-dione (I).* 1,10-Phenanthroline-5,6-dione was synthesized according to a modified literature procedure.<sup>45</sup>

1,10-Phenanthroline monohydrate (10 g, 50.4 mmol) was dissolved in small portions with stirring in 60 mL of concentrated sulfuric acid in a round-bottom flask. Sodium bromide (5.19 g, 50.4 mmol) was then added, followed by 30 mL of 70 wt % nitric acid. The flask was equipped with a reflux condenser, and the mixture was heated to 100 °C and kept at reflux temperature for 6 h. After 6 h, heating was reduced to 95 °C, and the reflux condenser was removed to allow bromine vapors to escape overnight. After being cooled, the mixture was poured onto 800 g of ice, carefully neutralized to pH = 7 with 10 M sodium hydroxide, and cooled to

(33) Li, H. R.; Lin, J.; Zhang, H. J.; Li, H. C.; Fu, L. S.; Meng, Q. G. *Chem. Commun.* **2001**, 13, 1212.

(34) Li, H. R.; Lin, J.; Fu, L. S.; Guo, J. F.; Meng, Q. G.; Liu, F. Y.; Zhang, H. J. *Microporous Mesoporous Mater.* **2002**, 55, 103.

(35) Li, H. R.; Lin, J.; Zhang, H. J.; Fu, L. S.; Meng, Q. G.; Wang, S. B. *Chem. Mater.* **2002**, 14, 3651.

(36) Li, H. R.; Fu, L. S.; Lin, J.; Zhang, H. J. *Thin Solid Films* **2002**, 416, 197.

(37) Franville, A. C.; Mahiou, R.; Zambon, D.; Cousseins, J. C. *Solid State Sci.* **2001**, 3, 211.

(38) Lenaerts, P.; Driesen, K.; Van Deun, R.; Binnemans, K. *Chem. Mater.* **2005**, 17, 2148.

(39) Lenaerts, P.; Ryckebosch, E.; Driesen, K.; Van Deun, R.; Nockemann, P.; Görlner-Walrand, C.; Binnemans, K. *J. Lumin.* **2005**, 114, 77.

(40) Carnall, W. T.; Goodman, G. L.; Rajnak, K.; Rana, R. S. *A schematic analysis of the spectra of the lanthanides doped into single-crystal LaF<sub>3</sub>*, ANL-88-8 report, Chemistry Division, Argonne National Laboratory, Argonne, IL, 1988.

(41) Davey, S. T.; France, P. W. *Br. Telecom. Technol. J.* **1989**, 7, 58.

(42) Voloshin, A. I.; Shavaleev, N. M.; Kazakov, V. P. *J. Lumin.* **2001**, 93, 199.

(43) Yu, J. Y.; Zhang, H.; Fu, L.; Deng, R. P.; Zhou, L.; Li, H. R.; Liu, F.; Fu, H. *Inorg. Chem. Commun.* **2003**, 6, 852.

(44) Filipescu, N.; Mushrush, G. W.; Hurt, C. R.; McAvery, N. *Nature* **1966**, 211, 960.

(45) Hiort, C.; Lincoln, P.; Norden, B. *J. Am. Chem. Soc.* **1993**, 115, 3448.

room temperature. The turbid solution was filtered. In the next step, the solids were extracted again 4–5 times with 200 mL of boiling water, and every time the turbid solution was filtered after being cooled to room temperature. The combined aqueous solutions were extracted with several portions of dichloromethane, dried over anhydrous magnesium sulfate, and evaporated under reduced pressure. The crystalline residue was recrystallized from 300 mL of toluene to give the pure dione. The product was dried in vacuo at 50 °C. Yield: 40% (4.6 g). Mp: 257 °C.  $\delta_{\text{H}}$  (300 MHz, DMSO- $d_6$ ): 7.58–7.62 (dd, 2H), 8.49–8.52 (dd, 2H), 9.11–9.13 (dd, 2H). Anal. Calcd for  $(\text{C}_{12}\text{H}_6\text{N}_2\text{O}_2)_3(\text{H}_2\text{O})_3$ : C, 66.67; H, 3.11; N, 12.96%. Found: C, 67.22; H, 2.97; N, 12.99%.

*Synthesis of 2-(4'-Hydroxyphenyl)imidazo[4,5-f]-1,10-phenanthroline (2).* The method used for the synthesis of 2-(4'-hydroxyphenyl)imidazo[4,5-f]-1,10-phenanthroline was similar to the method used by Steck and Day for the preparation of 2-substituted phenanthrimidazoles.<sup>46</sup>

1,10-Phenanthroline-5,6-dione (**1**) (1 g, 4.6 mmol) and ammonium acetate (5.86 g, 133 mmol) were dissolved in 10 mL of hot glacial acetic acid. While the mixture was stirred, a solution of 4-hydroxybenzaldehyde (0.565 g, 4.6 mmol) in 10 mL of glacial acetic acid was added dropwise to the mixture. The mixture was heated at 90 °C for 3 h and was then poured in 200 mL of water. The solution was neutralized with ammonia to pH = 7 and was then cooled to room temperature. The precipitate was filtered off and washed with large portions of water. The product was dried for 48 h in vacuo at 50 °C. Yield: 70% (1.1 g).  $\delta_{\text{H}}$  (300 MHz, DMSO- $d_6$ ): 6.95–7.13 (d, 2H), 7.77–7.88 (m, 2H), 8.08–8.15 (d, 2H), 8.86–8.93 (dd, 2H), 8.97–9.03 (dd, 2H), 10 (OH), 13.5 (NH). IR (KBr,  $\text{cm}^{-1}$ ): 3392 (stretch OH). MS (CI):  $m/z$  = 313 ( $\text{MH}^+$ ). Anal. Calcd for  $(\text{C}_{19}\text{H}_{12}\text{N}_4\text{O}_1)_2(\text{H}_2\text{O})_3$ : C, 67.24; H, 4.45; N, 16.51%. Found: C, 67.20; H, 4.61; N, 16.07%.

*Synthesis of 2-[4'-(3-(Triethoxysilyl)propyl)phenyl]imidazo[4,5-f]-1,10-phenanthroline (3).* An excess of 3-(triethoxysilyl)propyl isocyanate (4 mL, 14.9 mmol) was added to 2-(4'-hydroxyphenyl)imidazo[4,5-f]-1,10-phenanthroline (**2**) (0.100 g, 0.295 mmol). The mixture was kept under argon in an ultrasonic bath for a few minutes. Then, the mixture was stirred under argon at 80 °C for 72 h. The mixture was added dropwise to 30 mL of cold hexane, and a white-yellow precipitate was obtained. The precipitate was filtered off, washed with cold hexane, and then dissolved in ethanol. The solution was filtered, and the ethanol was removed by rotary evaporation. The compound was dissolved in a small portion of dichloromethane. This shows that reaction occurred, since the starting product is not soluble in dichloromethane. This solution was added dropwise to 30 mL of cold hexane to reprecipitate the compound. The purified product was filtered off and dried in vacuo. Yield: 67% (0.110 g).  $\delta_{\text{H}}$  (300 MHz, DMSO- $d_6$ ): 0.61 (t, 2H), 1.17 (t, 9H), 1.54–1.59 (m, 2H), 3.07–3.10 (m, 2H), 3.78 (q, 6H), 7.36 (d, 2H), 7.82–7.89 (m, 2H), 8.29 (d, 2H), 8.91 (dd, 2H), 9.04 (dd, 2H), 13.73 (NH).  $\delta_{\text{C}}$  (400 MHz, DMSO- $d_6$ ): 7.25, 18.21, 22.86, 43.24, 57.7, 119.31, 122.26, 123.11, 123.37, 123.75, 126.40, 126.73, 127.30, 129.56, 135.77, 143.54, 143.69, 147.79, 150.11, 152.24, 154.04. IR (KBr,  $\text{cm}^{-1}$ ): 1717 (C=O stretch). Anal. Calcd for  $(\text{C}_{29}\text{N}_5\text{O}_5\text{H}_{33}\text{Si}_1)_2(\text{H}_2\text{O})_3$ : C, 59.36; H, 6.18; N, 11.93%. Found: C, 59.26; H, 6.18; N, 11.63%.

*Synthesis of the Lanthanide(III) Complexes.* The  $[\text{Ln}(\text{tta})_3(\text{H}_2\text{O})_2]$  complexes were prepared for Ln = Pr, Nd, Sm, Eu, Dy, Ho, Er, Tm, Yb, according to the procedure described by Melby et al.<sup>47</sup> The purity of the compounds was verified by CHN elemental analysis.

The  $[\text{Eu}(\text{tta})_3(\text{phen})]$  complex that was used as the reference complex for the determination of the quantum yield was prepared according to the procedure described by Uekawa et al.<sup>48</sup> The purity of the compound was verified by CHN elemental analysis.

*Synthesis of the Lanthanide(III)-Doped Bulk Samples.*  $[\text{Ln}(\text{tta})_3(\text{H}_2\text{O})_2]$  (0.0606 mmol) and **3** (44.32 mg, 0.0755 mmol) were dissolved in 100 mL of ethanol. Part of this solution (16 mL) was mixed with tetramethoxysilane (TMOS, 12 mL), diethoxydimethylsilane (DEDMS, 4 mL), and water (4 mL). Glass vials (diameter: 24 mm, height: 48 mm) were filled with aliquots (1, 2, or 3 mL) of this solution and were covered with Parafilm. After 2 days, three small holes are pierced in the Parafilm. Monolithic glass samples were obtained after a drying period of 1 month. Before the luminescence measurements were made, the glass samples were dried for 48 h in an oven at 100 °C.

*Synthesis of the Lanthanide-Doped TMOS–DEDMS Thin Films.*  $[\text{Ln}(\text{tta})_3(\text{H}_2\text{O})_2]$  (0.1212 mmol) and **3** (88.64 mg, 0.151 mmol) were dissolved in 10 mL of ethanol. Part of this solution (8 mL) was mixed with tetramethoxysilane (TMOS, 4 mL), diethoxydimethylsilane (DEDMS, 4 mL), and water (2 mL). This composition is very similar to the one used for the bulk samples. Only the content of DEDMS was increased to 50% to improve the mechanical properties and to avoid cracks in the film,<sup>49,50</sup> and a higher concentration of the complex has been used. Glass vials (diameter 24 mm, height 48 mm) were filled with 9 mL of this solution and were covered with Parafilm. After 2 days, three small holes were pierced in the Parafilm. After 6 days, thin films were prepared from the partly hydrolyzed and condensed solution by spin-coating on small glass slides (width 8.5 mm; height 25 mm) to fit in a cuvette for the measurement of the quantum yields and on silicon wafers (width: 25 mm; height: 25 mm) for the SEM measurements. The substrates were cleaned first by putting them in distilled water with a surfactant. In the next step, they were cleaned ultrasonically for 30 min in distilled water with surfactant and then ultrasonically for 10 min in acetone, and finally they were boiled for 10 min in 2-propanol. Before spin-coating, the substrate was rinsed with 2-propanol and spun dry. Then, the partially hydrolyzed and condensed sol–gel solution was dropped on the substrate with a syringe through a 2  $\mu\text{m}$  filter and spin-coated at 2000 rpm for 30 s. The concentration of the luminescent complex is 20 times higher in the sol–gel solution that is used to prepare the thin film than in the precursor solution or the bulk samples. This is because otherwise the doping concentration in the thin film would be too low to obtain a sufficiently high luminescence output. During these experiments, we noticed that a higher concentration of complex in the sol–gel has a catalytic effect on the hydrolysis and condensation reactions. Therefore, also films with the same concentration in luminescent complex as the bulk samples were prepared in the same way as the more concentrated films, and the layer thicknesses of the films prepared from the different precursor solutions were compared. If the sol–gel precursor solution is less condensed, the solution will be less viscous, and thinner films are the result. Before the luminescence measurements, different drying methods have been used: under atmospheric conditions at RT (room temperature), in vacuo at RT, or at 50 °C in atmospheric conditions.

*Synthesis of the Lanthanide-Doped TMOS–GLYMO Thin Films.* For the second type of film, a similar precursor solution was prepared with 4 mL of 3-glycidoxypropyltrimethoxysilane instead of diethoxydimethylsilane. This composition was used because lanthanide(III)-doped xerogels with GLYMO are reported by

(46) Steck, E. A.; Day, A. R. *J. Am. Chem. Soc.* **1943**, *65*, 452.

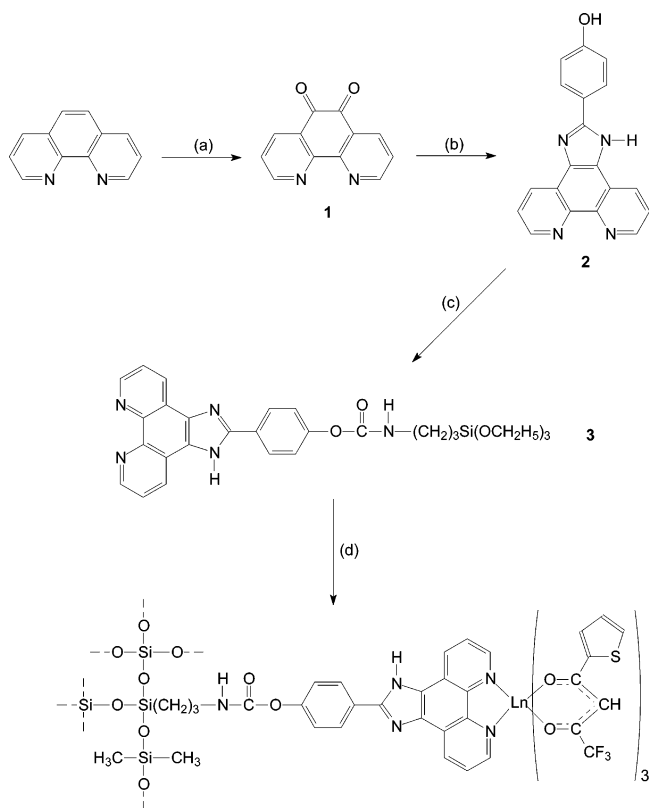
(47) Melby, L. R.; Rose, N. J.; Abramson, E.; Caris, J. C. *J. Am. Chem. Soc.* **1964**, *86*, 5117.

(48) Uekawa, M.; Miyamoto, Y.; Ikeda, H.; Kaifu, K.; Nakaya, T. *Bull. Chem. Soc. Jpn.* **1998**, *71*, 2253.

(49) Cao, B.; Zhu, C. *J. Non-Cryst. Solids* **1994**, *178*, 302.

(50) Tanner, P. A.; Yan, B.; Zhang, H. *J. Mater. Sci.* **2000**, *35*, 4325.

**Scheme 1. Synthesis of the Hydrolyzable Imidazo-1,10-phenanthroline Derivative and Preparation of the Lanthanide-Doped Inorganic–Organic Hybrid Sol–Gel Glass via the Sol–Gel Route<sup>a</sup>**



<sup>a</sup> Reagents and experimental conditions: (a)  $\text{HNO}_3/\text{H}_2\text{SO}_4$ ,  $\text{NaBr}$ ; (b) 4-hydroxybenzaldehyde,  $\text{CH}_3\text{COOH}$ ,  $\text{CH}_3\text{COONH}_4$ ; (c) 3-isocyanatopropyltriethoxysilane,  $80^\circ\text{C}$ , 72 h; (d) TMOS, DEDMS,  $\text{H}_2\text{O}$ , ethanol,  $[\text{Ln}(\text{tta})_3(\text{H}_2\text{O})_2]$ .

Reisfeld et al. to have a high luminescence efficiency.<sup>51</sup> In this case, the glass vials were also filled with 9 mL of the solution and covered with Parafilm. The TMOS–GLYMO solution turned out to reach the gel-point faster than the TMOS–DEDMS mixture. Therefore, holes were pierced in the Parafilm after only 1 day, and the TMOS–GLYMO solution was stored for only 2 days before spinning, while the TMOS–DEDMS mixture was stored for 6 days. After 2 days, thin films were prepared by spin-coating on small glass slides (width 8.5 mm; height 25 mm) and silicon wafers (width: 25 mm; height: 25 mm). The cleaning procedure and drying methods were similar to the TMOS–DEDMS thin films.

## Results and Discussion

The synthesis of the different organic precursors and of the lanthanide(III)-doped organic–inorganic hybrid materials is outlined in Scheme 1.

In the first step, 1,10-phenanthroline-5,6-dione (**1**) is formed by oxidation of 1,10-phenanthroline. The dione is transformed into the imidazo[4,5-*f*]-1,10-phenanthroline substituted in the 2-position by a 4-hydroxyphenyl group (**2**). By reaction of (**2**) with an excess of 3-(triethoxysilyl)propyl isocyanate, a hydrolyzable sol–gel precursor containing the imidazo[4,5-*f*]-1,10-phenanthroline moiety (**3**) is obtained.

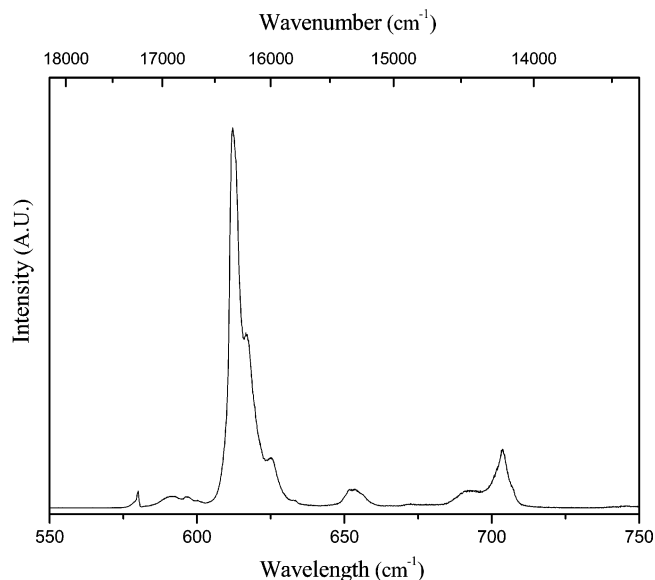


**Figure 1.** Emission spectrum for the covalently linked  $[\text{Eu}(\text{tta})_3(\text{phen})]$  complex in the bulk sol–gel glass. The excitation wavelength was 370 nm. All the transitions in the spectrum start from the  $^5\text{D}_0$  state and end at the  $^7\text{F}_j$  levels ( $J = 0-4$  for this spectrum).

Monolithic bulk samples with different lanthanide(III) ions have been prepared ( $\text{Ln} = \text{Pr}$ ,  $\text{Nd}$ ,  $\text{Sm}$ ,  $\text{Eu}$ ,  $\text{Dy}$ ,  $\text{Ho}$ ,  $\text{Er}$ ,  $\text{Tm}$ ,  $\text{Yb}$ ). The  $[\text{Ln}(\text{tta})_3(\text{H}_2\text{O})_2]$  complex was added to the TMOS–DEDMS precursors and the hydrolyzable imidazo-1,10-phenanthroline derivative (**3**). In this way, the coupled  $[\text{Ln}(\text{tta})_3(\text{phen})]$  complex can be formed in the organic–inorganic hybrid matrix. An excess of the 1,10-phenanthroline derivative was used in the sol–gel solution to ensure that all of the complex was attached to the matrix by the 1,10-phenanthroline. All bulk samples were dried at elevated temperatures ( $100^\circ\text{C}$ ) before luminescence measurements. Heating of the lanthanide(III)-doped sol–gel bulk sample is a general procedure to finalize all condensation reactions and eliminate water and ethanol.<sup>52–54</sup> For the bulk samples, no changes in the fine structure or intensities of the luminescence spectra were observed after the heating treatment. Influence of drying on the luminescence quantum yield will be discussed later in this paper.

The europium(III) ion was used as a spectroscopic probe to obtain evidence for the adduct formation, because the europium(III) complex shows an intense fine-structured emission band centered around 612 nm ( $^5\text{D}_0 \rightarrow ^7\text{F}_2$  transition) and this transition is very sensitive to small changes in the first coordination sphere. The emission spectrum of the europium(III)-doped sample is shown in Figure 1. The maximum excitation wavelength was at 370 nm.

When one zooms in on the  $^5\text{D}_0 \rightarrow ^7\text{F}_2$  transition and one compares the spectrum of the europium(III) complex in the sol–gel matrix to that of the pure  $[\text{Eu}(\text{tta})_3(\text{phen})]$  complex in a KBr pellet, it is evident that the positions of the crystal field transitions (612, 617, and 625 nm in both cases) and

(52) Li, H.; Inoue, S.; Machida, K.; Adachi, G. *Chem. Mater.* **1999**, *11*, 3171.

(53) Li, H. R.; Zhang, H. J.; Lin, J.; Wang, S. B.; Yang, K. Y. *J. Non-Cryst. Solids* **2000**, *278*, 218.

(54) Li, H.; Inoue, S.; Machida, K.; Adachi, G. *J. Lumin.* **2000**, *87–89*, 1069.

(51) Reisfeld, R.; Saraidarov, T.; Pietraszkiewicz, M.; Lis, S. *Chem. Phys. Lett.* **2001**, *349*, 266.

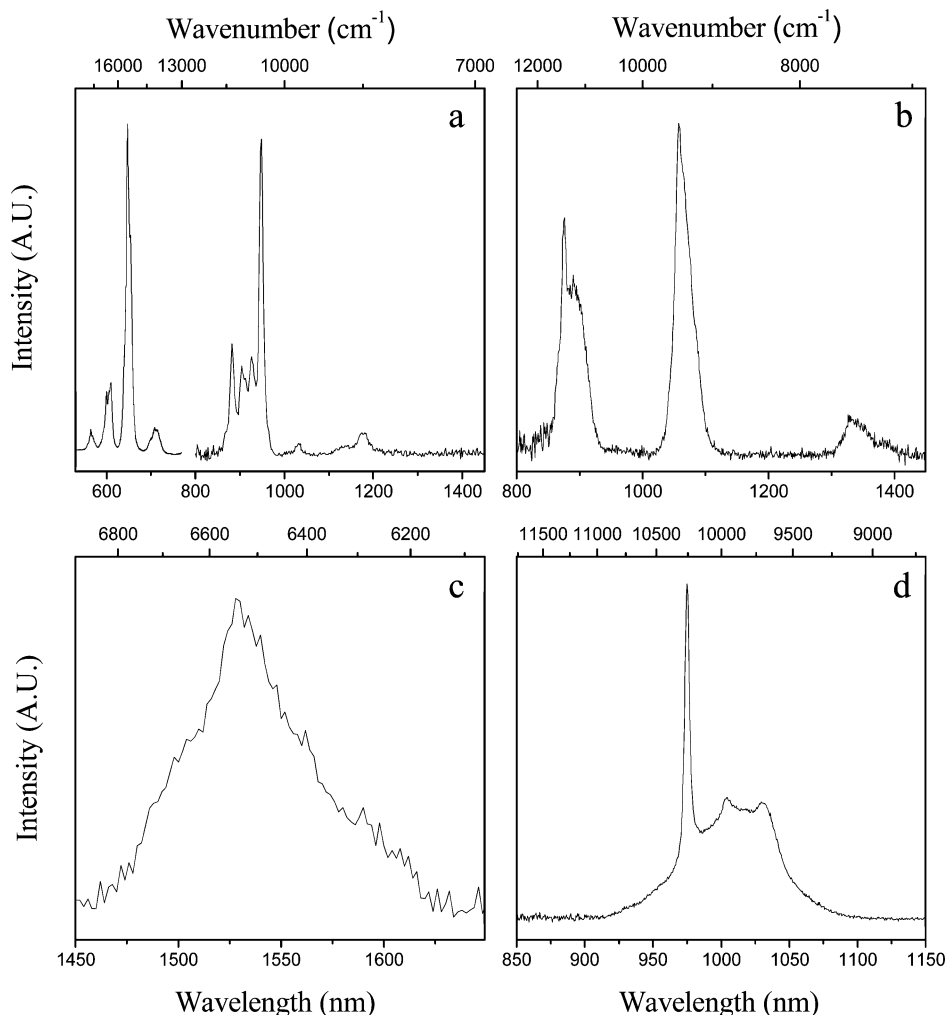


**Figure 2.** Emission spectra for the covalently linked  $[\text{Ln}(\text{tta})_3(\text{phen})]$  complexes in the TMOS–DEDMS sol–gel bulk sample. The excitation wavelength was 370 nm. (a)  $\text{Ln} = \text{Sm}$ . The transitions start from the  ${}^4\text{G}_{5/2}$  state and end at the  ${}^6\text{H}_J$  levels ( $J = 5/2-15/2$  for this spectrum) and the different  ${}^6\text{F}_J$  levels ( $J = 5/2-9/2$ ). (b)  $\text{Ln} = \text{Nd}$ . All transitions start from the  ${}^4\text{F}_{3/2}$  state and end at the  ${}^4\text{I}_J$  levels ( $J = 9/2-13/2$ ). (c)  $\text{Ln} = \text{Er}$ . The transition starts from the  ${}^4\text{I}_{13/2}$  level to the  ${}^4\text{I}_{15/2}$  level. (d)  $\text{Ln} = \text{Yb}$ . The transition starts from the  ${}^2\text{F}_{5/2}$  level to the  ${}^2\text{F}_{7/2}$  level.

the fine structure of the emission in the sol–gel matrix are very comparable to those of the pure complex. This shows that the linked  $[\text{Eu}(\text{tta})_3(\text{phen})]$  complex has been formed in the sol–gel matrix. In contrast, the fine structure of the  $[\text{Eu}(\text{tta})_3(\text{H}_2\text{O})_2]$  complex shows different peak positions (612, 614, and 619 nm).<sup>32,38</sup> Moreover, the observed lifetime of  $\text{Eu}^{3+}$  is shorter in the  $[\text{Eu}(\text{tta})_3(\text{H}_2\text{O})_2]$  complex (190  $\mu\text{s}$ ) than in the sol–gel matrix (600  $\mu\text{s}$ ). This can be explained by the fact that the water molecules in the first coordination sphere of  $[\text{Eu}(\text{tta})_3(\text{H}_2\text{O})_2]$  provide an efficient route for radiationless deactivation, and this supports the hypothesis that, in the sol–gel glass, the europium(III) ion is present in  $[\text{Eu}(\text{tta})_3(\text{phen})]$  which is covalently attached to the silica matrix. In the spectrum, there is no evidence for emission from the triplet state of the imidazo[4,5-*f*]-1,10-phenanthroline or the 2-thenyltrifluoroacetate ligands. This indicates that there is an efficient energy transfer from the triplet states of the organic ligands to the central europium ion. The efficient energy transfer from imidazo[4,5-*f*]-1,10-phenanthroline molecules was also determined previously by Gao et al.<sup>55</sup>

If other lanthanide complexes are introduced in the sol–gel bulk sample, both visible and near-infrared signals could be detected. After addition of  $[\text{Sm}(\text{tta})_3(\text{H}_2\text{O})_2]$  to the sol–gel precursor solution, the  $[\text{Sm}(\text{tta})_3(\text{phen})]$  complex was formed in the hybrid material. The spectra in the visible and near-infrared region are shown in Figure 2a. In the visible region, the  ${}^4\text{G}_{5/2} \rightarrow {}^6\text{H}_{9/2}$  transition at 648 nm is the most intense. The observed lifetime for this transition was 55  $\mu\text{s}$ . In the near-infrared region, the  ${}^4\text{G}_{5/2} \rightarrow {}^6\text{F}_{5/2}$  transition at 950 nm is the most intense, and the lifetime was 40  $\mu\text{s}$ . The spectra of other  $[\text{Ln}(\text{tta})_3(\text{phen})]$  complexes ( $\text{Ln} = \text{Nd}, \text{Er}, \text{Yb}$ ) that are known to exhibit intense near-infrared luminescence are shown in Figure 2b–d. The observed lifetime for the neodymium(III)-doped sample was 0.32  $\mu\text{s}$ , for the erbium(III)-doped sample 0.95  $\mu\text{s}$ , and for the ytterbium(III)-doped bulk sol–gel 12  $\mu\text{s}$ .

Also, less-frequently investigated  $[\text{Ln}(\text{tta})_3(\text{phen})]$  complexes ( $\text{Ln} = \text{Pr}, \text{Dy}, \text{Ho}, \text{Tm}$ ) were introduced in the TMOS–DEDMS sol–gel glass. No signals could be observed for the samples containing dysprosium(III) and thulium(III). However, for the sol–gel glasses with praseodymium(III) and holmium(III) complexes, transitions have been observed in the luminescence spectra. The spectra of  $[\text{Pr}$

(55) Gao, D.; Bian, Z. Q.; Wang, K. Z.; Jin, L. P.; Huang, C. H. *J. Alloys Compd.* **2003**, *358*, 188.

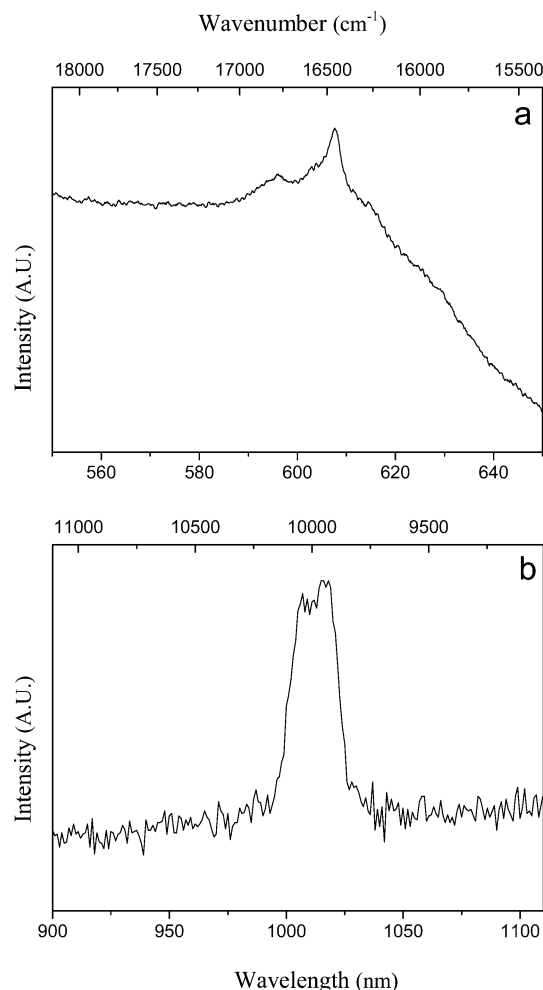


**Figure 3.** Emission spectra in (a) the visible region and (b) the near-infrared region of the TMOS–DEDMS praseodymium(III)-doped sol–gel bulk sample. In the visible region, the transition starts from the  $^1D_2$  state and ends at the  $^3H_4$  level. In the near-infrared region, the transition starts from the  $^1D_2$  level to the  $^3F_4$  level. The excitation wavelength is 370 nm. The spectrum in the near-infrared region was recorded at 77 K.

(tta)<sub>3</sub>(phen)] in the TMOS–DEDMS bulk sol–gel matrix are shown in Figure 3. It can be noticed from Figure 3a that Pr<sup>3+</sup> with 2-thenoyltrifluoroacetate and 1,10-phenanthroline in the sol–gel shows only weak luminescence in the visible region. The weak  $^1D_2 \rightarrow ^3H_4$  transition is superimposed on the ligand emission. Ligand emission was also observed for the [Pr(tta)<sub>3</sub>(H<sub>2</sub>O)<sub>2</sub>] complex dissolved in DMSO.<sup>42</sup> In the hybrid matrix, the ligand emission was even more pronounced, because an excess of the phenanthroline derivative has been added to the sol–gel precursor solution to be sure that all of the complex has been covalently coupled to the matrix. The  $^1D_2 \rightarrow ^3F_4$  transition in the near-infrared region at 1013 nm (10100 cm<sup>-1</sup>) is shown in Figure 3b and was observed when the praseodymium(III)-doped sol–gel glass was cooled to 77 K. The signal was rather low, because of the ligand luminescence noticed in the spectrum of the visible region. No decay time could be measured for the Pr<sup>3+</sup> sample, because the signals were not intense enough to give reliable results.

Of importance is the observation of lanthanide-centered near-infrared luminescence in holmium(III) complexes which is shown in Figure 4. To the best of our knowledge, the near-infrared luminescence of a molecular holmium complex was

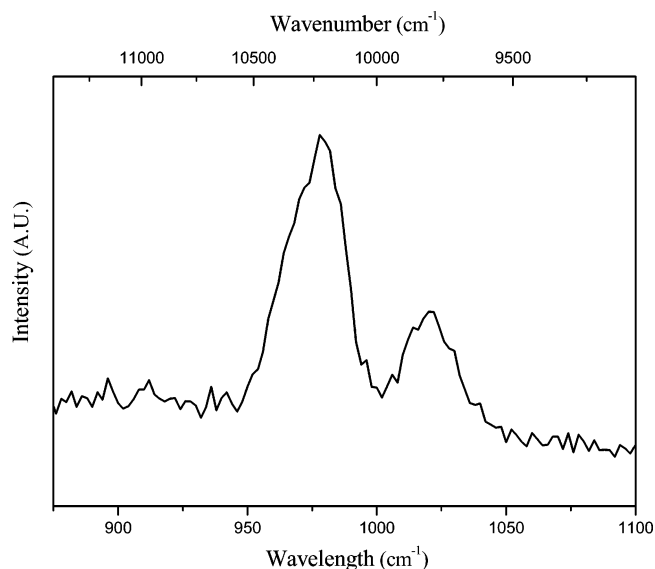


**Figure 4.** Emission spectrum of the holmium(III)-doped bulk sample. The transition starts from the  $^5S_2$  level to the  $^5I_6$  level. The excitation wavelength is 370 nm.

only described recently by Petoud and co-workers, who reported metal-centered luminescence for a holmium(III) tropolonate complex,<sup>56</sup> and by Quici and co-workers, who reported luminescence for a holmium(III) complex containing a single 1,10-phenanthroline chromophore and a diethylenetriamine tetracarboxylate unit as a lanthanide coordination site.<sup>57</sup> However, no reliable decay time could be measured for the Ho<sup>3+</sup> sample due to the weakness of the signal.

Although the sol–gel bulk samples show good luminescence properties, thin films of those materials have several advantages. For reproducible quantum yield measurement, the absorbance of the sample at the excitation wavelength has to be around 0.5, a condition which is difficult to fulfill for bulk samples. In addition, the position of the sample in the integrating sphere is very important. Therefore, thin films deposited on small glass slides (width 8.5 mm; height 25 mm) that just fit in a 1 cm quartz cuvette have been prepared. In this way, the position of the film in the integrating sphere is very reproducible. Even if low concentration bulk samples are used for the determination of the quantum yield, problems will rise with the positioning of the samples because of their irregular shape. To the best of our knowledge, this is the first time that quantum yields of europium complexes were determined directly on thin films with an integrating sphere and not by comparison of relative luminescence intensities<sup>42,51,52</sup> or indirectly by luminescence lifetime measurement.<sup>58,59</sup> Quantum yields of Nd<sup>3+</sup> and Er<sup>3+</sup> are typically below 0.1% which is lower than the detection limit of our setup. Another advantage of the thin films is the short drying time.<sup>60</sup> Drying times in bulk samples are long (at least 1

(56) Zhang, J.; Badger, P. D.; Geib, S. J.; Petoud, S. *Angew. Chem., Int. Ed.* **2005**, *44*, 2508.

(57) Quici, S.; Cavazzini, M.; Marzanni, G.; Accorsi, G.; Armaroli, N.; Ventura, B.; Barigelletti, F. *Inorg. Chem.* **2005**, *44*, 529.

(58) Magennis, S. W.; Ferguson, A. J.; Bryden, T.; Jones, T. S.; Beeby, A.; Samuel, I. D. W. *Synth. Met.* **2003**, *138*, 463.

(59) Shavaleev, N. M.; Moorcraft, L. P.; Pope, S. J. A.; Bell, Z. R.; Faulkner, S.; Ward, M. D. *Chem. Eur. J.* **2003**, *9*, 5283.

(60) Brinker, C. J.; Scherer, G. W. *Sol-Gel Science*; Academic Press: San Diego, CA, 1990; p 798.

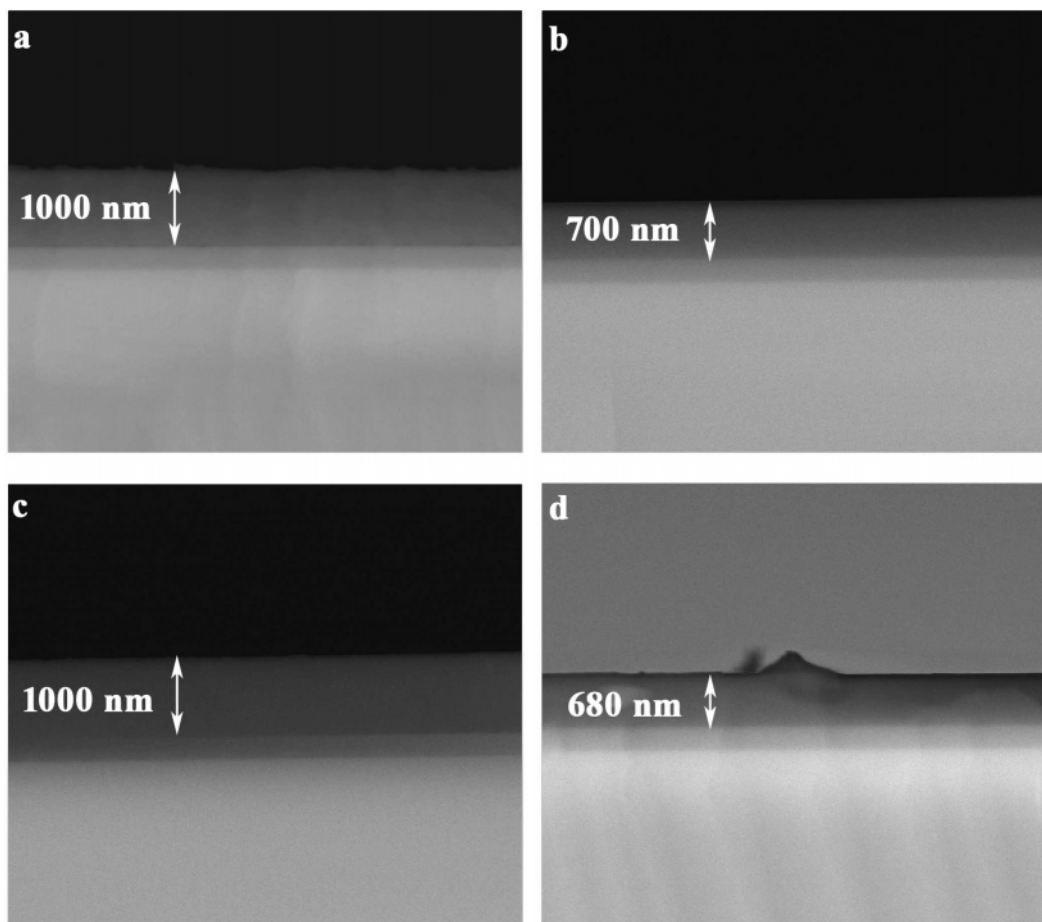


**Figure 5.** SEM cross section images on (a) the high concentration TMOS–DEDMS thin film, (b) the low concentration TMOS–DEDMS thin film, (c) the high concentration TMOS–GLYMO thin film, and (d) the low concentration TMOS–GLYMO thin film.

**Table 1. Characteristics of Sol–Gel Films Doped with [Eu(tta)<sub>3</sub>(phen)]**

composition	concentration <sup>a</sup> (10 <sup>-4</sup> M)	gelation time before spinning (days)	film thickness (nm)
TMOS–DEDMS (50:50)	2.7	6	700
TMOS–DEDMS (50:50)	53.8	6	1000
TMOS–GLYMO (50:50)	2.7	2	680
TMOS–GLYMO (50:50)	53.8	2	1000

<sup>a</sup> Concentration of the complex in the starting precursor solution.

month). Thin films are also more suitable for applications. Therefore, thin films containing europium(III), neodymium(III), and erbium(III) complexes have been prepared by the spin-coating process on glass slides or oxidized silica wafers. An overview of the layer thicknesses of the europium(III)-doped films is given in Table 1.

By analyzing the layer thickness, it is evident that the sol–gel solutions with higher concentration of the complex were more viscous in the same conditions than in the less concentrated mixtures. A more viscous solution results in a thicker film. This was expected by observation of the gelation times of the bulk samples with the same composition. The lanthanide complex seems to have a catalytic effect on the hydrolysis and condensation reactions in the silica sol–gel procedure. It was also clear that the sol–gel with TMOS–GLYMO undergoes faster condensation than the one with TMOS–DEDMS. The SEM cross-section images of the TMOS–DEDMS films and the TMOS–GLYMO films are

**Table 2. Quantum Yields on the Sol–Gel Films after Different Drying Methods**

composition	drying method	quantum yield (%)
TMOS–DEDMS	1 week in atmosphere	27 ± 2
	3 weeks in atmosphere	26 ± 2
	+ 48 h in vacuo	27 ± 2
	+ 48 h 50 °C	12 ± 2
	+ 1 week 50 °C	12 ± 2
TMOS–GLYMO	1 week in atmosphere	34 ± 2
	3 weeks in atmosphere	34 ± 2
	+ 48 h in vacuo	33 ± 2
	+ 48 h 50 °C	26 ± 2
	+ 1 week 50 °C	26 ± 2

shown in Figure 5. Before SEM measurements, the films were dried for 1 week in atmospheric conditions and then for 2 days in vacuo.

The films prepared in this way had an absorbance of 0.4 and were appropriate for the determination of quantum yields with the integrating sphere. Europium(III) is the most suitable lanthanide ion for quantum yield measurements because it has a very intense luminescence transition around 612 nm and because appropriate reference complexes are available (e.g., [Eu(tta)<sub>3</sub>(phen)] in DMF,  $\phi = 36.5\%$ ).<sup>44</sup> Quantum yields were measured after drying in atmospheric conditions, after drying in vacuo, and after a heating treatment at 50 °C. The results were obtained by averaging at least three measurements and are summarized in Table 2.

It is evident from Table 2 that the quantum yields remained stable on the atmospheric dried TMOS–DEDMS films for

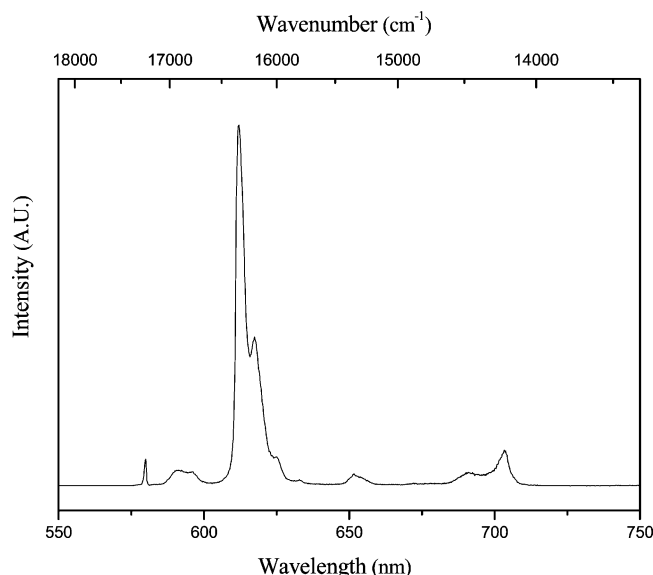


**Figure 6.** Emission spectrum for the covalently linked  $[\text{Eu}(\text{tta})_3(\text{phen})]$  complex in the TMOS-DEDMS thin film. The excitation wavelength was 341 nm. All the transitions in the spectrum start from the  $^5\text{D}_0$  state and end at the  $^7\text{F}_j$  levels ( $J = 0-4$  for this spectrum).

longer periods (27%). The quantum yield was also stable if the films were dried in vacuo for 48 h. A decrease to 12% was observed after heating at 50 °C, but no further decrease of the quantum yield was noticed if the films were heated at 50 °C for a longer time. A similar decrease of the quantum yield at higher temperatures was already observed by Li et al. by comparing luminescence intensities at elevated temperatures.<sup>52</sup> Measurement of the quantum yield is, however, a more exact method for detecting changes in luminescence efficiency. The observed lifetimes before and after drying are similar, indicating that the lanthanide ion itself is well shielded from its environment and only slightly influenced by changes in the matrix caused by drying at higher temperature. The ligands can be more sensitive to this drying procedure. The energy transfer process from the triplet level of the ligands to the emitting level of the lanthanide ion is different if the film is not exposed to elevated temperatures. A prolonged drying period has no further influence. Because of the decrease of the luminescence efficiency after drying at higher temperatures, we preferred to dry the thin films for 48 h in vacuo. In this way, all remaining solvents were removed from the thin film. The high quantum yield for the TMOS-GLYMO film (34%) is remarkable. This good luminescence was also established by Reisfeld et al.<sup>51</sup> By measurement of the relative luminescence intensities of europium(III)dibenzoylmethane complexes in zirconia xerogels with GLYMO, they had clear indications that the europium chelate has better spectroscopic properties in a zirconia-GLYMO film than in a film prepared of neat zirconia. This is due to a better energy transfer process in the GLYMO-modified material. The quantum yield of this europium(III)-doped film showed the same behavior as the TMOS-DEDMS thin film and remained very stable at room temperature or when dried in vacuo. After the heating procedure at 50 °C, the quantum yield decreased to 26%.

The luminescence spectrum of the europium(III)-doped film looks very much the same as those from the bulk samples of both the TMOS-DEDMS and TMOS-GLYMO compositions. The spectrum of the europium(III)-doped thin film is shown in Figure 6.

Small changes were noticed in the excitation spectrum. The maximum in the excitation spectrum of a bulk sol-gel glass is at 370 nm ( $27000\text{ cm}^{-1}$ ) while the excitation maximum in the thin film is at 341 nm ( $29300\text{ cm}^{-1}$ ), which corresponds to the maximum value in the absorption spectrum of the 2-thenoyltrifluoroacetate ligand. This can be explained by the fact that absorption at 341 nm in the bulk samples is very strong and part of the incident light beam at this wavelength will be absorbed only in the first part of the sample while excitation light at 370 nm will be absorbed throughout the bulk glass. This causes a higher peak in the excitation spectra of the bulk samples at 370 nm. The observed lifetime in the europium(III)-doped films (TMOS-DEDMS and TMOS-GLYMO) was  $600\ \mu\text{s}$ . For the neodymium(III)-doped TMOS-DEDMS film, the observed lifetime was  $0.31\ \mu\text{s}$  while for the erbium(III)-doped thin TMOS-DEDMS film a value of  $1.00\ \mu\text{s}$  was measured. Luminescence spectra for both near-infrared films are similar to the spectra observed in the bulk samples.

## Conclusions

In this paper, we show the use of a substituted imidazo[4,5-*f*]-1,10-phenanthroline moiety to attach highly luminescent lanthanide  $\beta$ -diketonate complexes to silica hybrid materials. The organic-inorganic hybrid matrix can be processed into thin films by spin-coating. The imidazo[4,5-*f*]-1,10-phenanthrolines are stable, easily accessible, and versatile building blocks. They are versatile, because 4-hydroxybenzaldehyde which is used to prepare the substituted imidazole ring can be replaced by other functionalized aldehydes. Additionally, the imidazole ring can be alkylated or even quaternized. The luminescence performance of the lanthanide complexes in the thin films of the silica hybrid material is very good. In particular, the europium(III) complex is highly luminescent, but also for other lanthanide complexes luminescence could be detected. Of importance here is the observation of lanthanide-centered near-infrared luminescence in praseodymium(III), samarium(III), and holmium(III) complexes.

**Acknowledgment.** P.L. is indebted to the Institute for the Promotion of Innovation by Science and Technology in Flanders (IWT-Vlaanderen) for financial support. K.B. and K.D. are Postdoctoral Fellows of the F.W.O.-Flanders (Belgium). Financial support by the F.W.O.-Flanders (G.0117.03), by the K.U.Leuven (GOA 03/03), and by the EU (GROWTH No: GRD2-2000-30346 OPAMD) is gratefully acknowledged. The research was partly performed in the framework of projects 1.2.16/D2/841 and 1.2.14/PO/841 of the Objective 2 programme for Limburg (Belgium) of the European Regional Development Fund. We thank Ms. Leen Van Nerum for measuring the mass spectra and for performing the CHN microanalyses.

CM051133S